The diverse evolutionary paths of simulated high-z massive, compact galaxies to $z = 0$

Sarah Wellons[1][*], Paul Torrey[2,3], Chung-Pei Ma[4], Vicente Rodriguez-Gomez[1],
Annalisa Pillepich[1], Dylan Nelson[1], Shy Genel[5][†], Mark Vogelsberger[2], and Lars Hernquist[1]

[1]*Harvard-Smithsonian Center for Astrophysics, 60 Garden St., Cambridge, MA 02138, USA*
[2]*Massachusetts Institute of Technology, Cambridge, MA 02139, USA*
[3]*TAPIR, Mailcode 350-17, California Institute of Technology, Pasadena, CA 91125, USA*
[4]*University of California Berkeley, Berkeley, CA 94720, USA*
[5]*Department of Astronomy, Columbia University, 550 West 120th Street, New York, NY, 10027, USA*

10 July 2015

ABSTRACT

Massive quiescent galaxies at high redshift have been observed to have much smaller physical sizes than their local counterparts. Several mechanisms have been invoked to explain the strong evolution of galaxy size with redshift, including progenitor bias, major and minor mergers, adiabatic expansion, and renewed star formation. However, it is difficult to connect galaxy populations between cosmological epochs to test these theories observationally. Herein, we select a sample of 35 massive, compact galaxies ($M_* = 1 - 3 \times 10^{11}$ M$_\odot$, $M_*/R^{1.5} > 10^{10.5}$ M$_\odot$/kpc$^{1.5}$) at $z = 2$ in the cosmological hydrodynamical simulation Illustris and trace them forward to $z = 0$ to uncover how they evolve to the present day. By $z = 0$, the original factor of 3 difference in stellar mass has spread to a factor of 20. The spread in dark matter halo mass similarly increases from a factor of 5 to a factor of 40. The compact galaxies' evolutionary paths are diverse: about half acquire an ex-situ envelope and exist as the core of a more massive descendant, 30% survive undisturbed and gain very little mass, 15% are entirely consumed and destroyed in a merger with a more massive galaxy, and the remainder are thoroughly mixed by major mergers. Nearly all the galaxies grow in size as well as mass, so that only about 10% of the $z = 2$ compact galaxies still satisfy our compactness criterion by $z = 0$. The majority of the size growth is driven by the acquisition of additional stellar mass at large radii through mergers and accretion. We find a relationship between a galaxy's $z = 0$ stellar mass and its progenitors' maximum past compactness: more massive galaxies are more likely to have had a compact progenitor. However, this trend possesses significant dispersion which precludes a direct linkage between massive galaxies at $z = 0$ and compact galaxies at $z = 2$. We find that a galaxy's $z = 2$ environment influences its merger rate and therefore its $z = 0$ outcome, so that isolated or satellite galaxies (which are protected from mergers) are the most likely to survive to the present day as compact relics.

Key words: galaxies: high-redshift, galaxies: evolution

1 INTRODUCTION

Massive galaxies at high redshift have been observed to have properties which can be quite different from their counterparts at similar mass in the local universe. One of the most striking differences is the much smaller sizes observed for high-redshift galaxies. For example, a quiescent galaxy with a stellar mass of 10^{11} M$_\odot$, which has a typical effective radius of 8 kpc in the local universe, has a typical size of only 1.7 kpc at $z = 2$ (van der Wel et al. 2014). Early reports of these extremely small sizes based on their spatial

extent (Daddi et al. 2005; van Dokkum et al. 2006; Trujillo et al. 2006) have been confirmed by dynamical measurements of their stars (van Dokkum, Kriek & Franx 2009; Cappellari et al. 2009; Newman et al. 2010; Belli, Newman & Ellis 2014) and, more recently, gas (Barro et al. 2014b; Nelson et al. 2014), in addition to higher-resolution HST imaging (van Dokkum et al. 2008; Szomoru, Franx & van Dokkum 2012; Williams et al. 2014). Several observational studies have tracked the strong evolution of galaxy size with redshift (Trujillo et al. 2007; Franx et al. 2008; Taylor et al. 2010; van der Wel et al. 2014), which is present in both star-forming and quiescent galaxies but is particularly dramatic in the latter case.

Part of the observed trend in median size is due to the continual addition of new, larger galaxies to the massive, quiescent

population. Star-forming disks have larger sizes at later times (Mo, Mao & White 1998). As these galaxies quench, their appearance in the quiescent population can shift the median size without changing the number density of compact galaxies, a phenomenon known as "progenitor bias" (van Dokkum & Franx 2001; Carollo et al. 2013). Careful accounting suggests that progenitor bias alone is insufficient to explain the observed size growth, however (Belli et al. 2014; Keating et al. 2015), so that the growth of individual galaxies within the quiescent population is also required. Recently, some authors have found that compact galaxies may not be as rare in the local universe as previously thought (Damjanov et al. 2014, 2015; Saulder, van den Bosch & Mieske 2015), suggesting that they must continue to be produced to replace those which "size out" of the compact selection.

Several authors have proposed mechanisms for increasing galaxies' sizes after quenching. Dry mergers between galaxies of similar masses increase size as $R_e \propto M$ (Hernquist, Spergel & Heyl 1993; Boylan-Kolchin, Ma & Quataert 2006; Hopkins et al. 2009b), while minor mergers may increase the sizes even more efficiently, $R_e \propto M^{>1}$ (Naab, Johansson & Ostriker 2009; Hopkins et al. 2010). In the latter case, it has been suggested that the massive, compact galaxies at high redshift now lie at the centers of the most massive galaxies in the local universe, having accreted a substantial amount of stellar mass since their initial formation (Hopkins et al. 2009a; van Dokkum et al. 2014) or regrown a star-forming disk (Graham, Dullo & Savorgnan 2015). This idea is supported by the observational fact that massive galaxies' interior densities evolve much less strongly than their overall size (Bezanson et al. 2009). The observed minor merger rate, however, may be too low to be entirely responsible for galaxies' growth (Newman et al. 2012). In the absence of mergers and accretion, galaxies may also "puff up" due to adiabatic expansion in response to the expulsion of gas from the inner regions from stellar winds and black hole feedback as $R_e \propto M^{-1}$ (Fan et al. 2008, 2010).

These attempts to explain what happens to high-redshift compact galaxies are hindered by the long timescales of galactic evolution, which limit observations of any individual system to a single evolutionary state. As a result, galaxy populations can only be connected at different epochs in a statistical sense. Simulations of galaxy formation, however, offer the opportunity to directly "observe" the evolution of individual systems over time. Large-volume simulations, moreover, can provide a cosmological context for that evolution and produce populations of galaxies which can be compared against observations.

In Wellons et al. (2015), we identified a set of galaxies in the cosmological hydrodynamical simulation Illustris which are analogs to observed massive compact ellipticals, with stellar masses of $1 - 3 \times 10^{11}$ M$_\odot$ and stellar half-mass radii of 2 kpc or smaller at $z = 2$. These compact galaxies formed naturally within the cosmological volume alongside non-compact galaxies at similar stellar masses, and we traced their progenitors back to higher redshift to discover how their formation paths differed. We found that the galaxies all reached their compact state through some combination of assembling their stellar mass at very early times when the universe was extremely dense, and/or intense, centralized bursts of star formation usually triggered by gas-rich mergers. Both in our work and in that of other simulators (see e.g. zoom-in simulations by Ceverino et al. (2015) and Zolotov et al. (2015)), gas-rich environments are required to dissipate angular momentum and produce such compact objects.

We now turn our attention to the low-redshift outcomes of these massive, compact galaxies. As before, we identify a massive, compact population at $z = 2$ in Illustris, this time tracing the galaxies forward to $z = 0$. In Section 2, we describe the Illustris simulation suite and the merger trees used to connect galaxies at different redshifts. In Section 3, we select a population of 35 compact galaxies at $z = 2$ and follow them forward to their $z = 0$ descendants. In Section 4, we take a detailed look at four distinct types of descendants and show how common each type of evolutionary track is, and in Section 5 we discuss how a galaxy's $z = 2$ environment might influence its eventual outcome. Finally, in Section 6 we address the likelihood of massive galaxies in the local universe hosting compact cores, explore the different mechanisms for size growth, and discuss the implications for the number density of compact galaxies at low redshift. We summarize the results and conclude in Section 7.

2 ILLUSTRIS

Illustris (Vogelsberger et al. 2014a,b; Genel et al. 2014; Nelson et al. 2015) is a cosmological hydrodynamical simulation with a periodic volume of $(106.5 \text{ Mpc})^3$ that is initialized at $z = 127$ using cosmological intial conditions and evolved forward to the present day. The simulation suite consists of 6 runs in total: 3 different levels of resolution, each run once with dark matter particles only and once with full baryonic physics, including gas cells, stellar and wind particles, and black hole particles. The results presented in this paper are drawn from the highest-resolution full-physics run, Illustris-1, which has a baryonic mass resolution element of about 10^6 M$_\odot$. The gravitational forces exerted by DM and star particles are softened on a comoving scale of $\epsilon = 1.4$ kpc. For gas cells, the force softening is spatially adaptive with cell volume. For all baryonic resolution elements (including both star particles and gas), ϵ is limited to a maximum physical size of 0.7 kpc at $z = 1$.

In addition to gravity, the full-physics runs in Illustris include a hydrodynamical treatment of gas using the moving-mesh code AREPO (Springel 2010) and models for the baryonic physical processes that regulate the growth of stellar mass. These include primordial (Katz, Weinberg & Hernquist 1996) and metal-line gas cooling (Wiersma, Schaye & Smith 2009) with self-shielding corrections (Rahmati et al. 2013), star formation and evolution, supernova feedback (Springel & Hernquist 2003), chemical enrichment of the ISM (Wiersma et al. 2009), and supermassive black hole growth with quasar-mode (Di Matteo, Springel & Hernquist 2005; Springel, Di Matteo & Hernquist 2005) and radio-mode feedback (Sijacki et al. 2007, 2014). These models are described in detail by Vogelsberger et al. (2013) and Torrey et al. (2014), who show that they produce realistic galaxy populations and reproduce key observables across cosmological time.

The SUBFIND algorithm (Springel et al. 2001; Dolag et al. 2009) is employed to identify gravitationally-bound structures (i.e. DM halos and subhalos) within the simulation volume. Their baryonic components (gas, stars, and black holes) comprise the galaxies that inhabit each subhalo.

Subhalos are tracked from snapshot to snapshot using the SUBLINK merger trees developed by Rodriguez-Gomez et al. (2015). A subhalo's potential descendants in the following snapshot are identified by shared ownership of individual particles (DM, stars, and gas). The particles are ranked according to gravitational binding energy and weighted according to $(\text{rank})^{-1}$. The subhalo with the highest weighted sum over all shared particles is then assigned as the descendant. A merger occurs when two or more subhalos share a common descendant. The main (or primary) progeni-
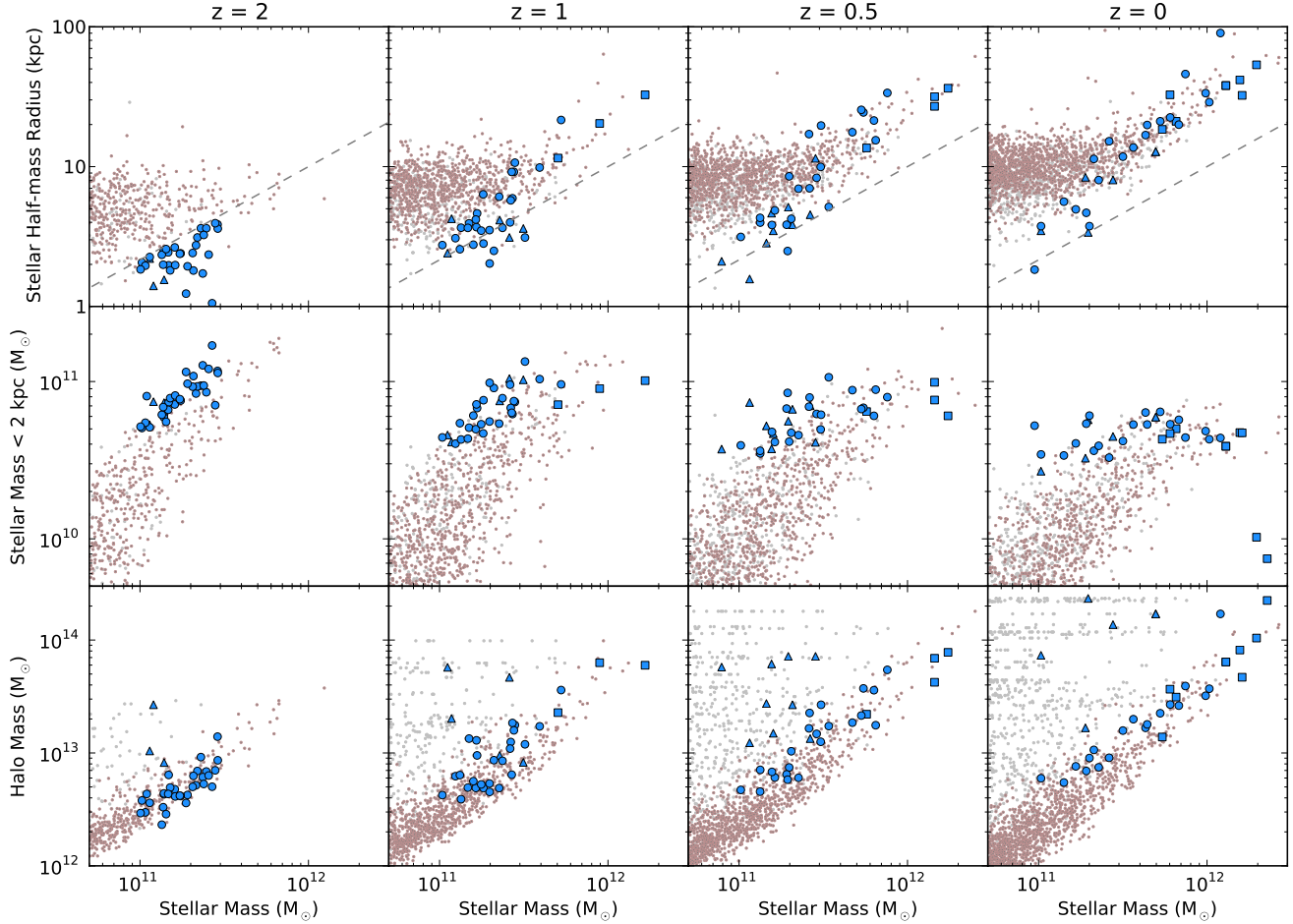
Figure 1. Evolution of the $z = 2$ compact population to the present day. Throughout, the compact galaxies' descendants are shown in blue symbols. Triangles indicate satellite galaxies at the current redshift, and squares indicate that the compact galaxy is not in the main progenitor branch of its descendant's merger tree (i.e., that it merged with a more massive galaxy). The remainder of the massive galaxy population is shown in dark pink and light grey points indicating central and satellite galaxies respectively. *Top row:* Size-mass plane at z=2, 1, 0.5, and 0. The $\log(\Sigma_{1.5}) > 10.5$ compactness selection criteria is represented by a dashed grey line. *Middle row:* Total stellar mass within 2 (physical) kpc of the galaxy center. *Bottom row:* Stellar mass - halo mass. For satellite galaxies, the halo mass shown is that of the FOF group to which it belongs, so that it lies to the left of its central galaxy. The compact galaxies' descendants spread out by a factor $\geqslant 6$ in both stellar mass and halo mass but remain some of the densest cores in the simulation.

tor of this descendant is chosen according to which subhalo has the "most massive history" (De Lucia & Blaizot 2007), which protects against the misallocation of particles that can occur when subhalos are close to merging. We traverse this merger tree forward in time to find the low-redshift descendants of our compact galaxies.

3   SAMPLE SELECTION AND OVERALL EVOLUTION

We quantify "compactness" using the observationally-motivated (see e.g. Barro et al. 2013) quantity

$$\Sigma_{1.5} = M_*/R^{1.5} \qquad (1)$$

where M_* is a galaxy's stellar mass and R its size. This constitutes a diagonal cut across the mass-radius plane so that lower-mass galaxies must have smaller sizes in order to qualify as compact. We use subhalo stellar masses and stellar half-mass radii to select a

population of galaxies at $z = 2$ with

$$\log \left(\frac{\Sigma_{1.5}}{M_\odot/kpc^{1.5}} \right) > 10.5 \qquad (2)$$

and stellar masses of $1 - 3 \times 10^{11}$ $M_\odot$, consisting of 35 galaxies in total. This selection differs from (and is more generous than) the strict 2 kpc size threshold imposed in Wellons et al. (2015). With this $\Sigma_{1.5}$ criterion, a galaxy of 10^{11} $M_\odot$ must still have a size of approximately 2 kpc or below, but we now allow larger sizes at higher masses so the total size of the compact population is more than doubled from the previous work. (The original 14 galaxies are a subsample of the 35 galaxies we examine here.) The selection criteria and resulting compact population are shown on the $z = 2$ size-mass plane in the upper left-hand panel of Figure 1. Two-thirds of the compact galaxies thus selected are quiescent (sSFR $< 3 \times 10^{-10}$/yr) at $z = 2$, which is a broadly similar fraction to observations (Barro et al. 2014a; van Dokkum et al. 2015).

Note that our definition of $\Sigma_{1.5}$ is slightly different from observers', since we use stellar half-mass radius (a three-dimensional
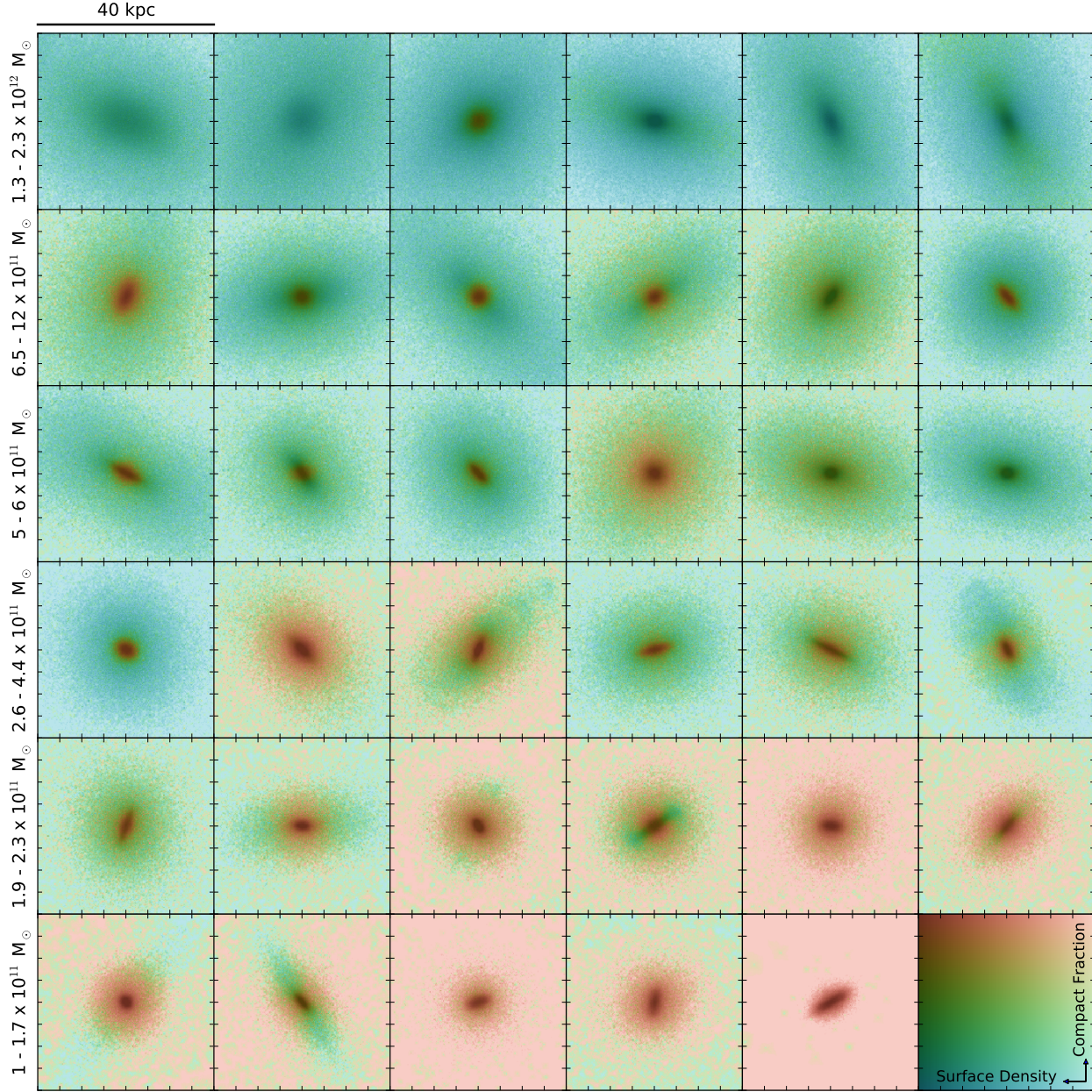
Figure 2. Images of the $z = 0$ descendants of each of the $z = 2$ compact galaxies, ordered by descendant mass. A color's intensity is determined by stellar surface density, and its hue by what fraction of the stars along the line of sight belong to the compact progenitor at $z = 2$ (legend in bottom right). Thus the least massive descendants which have primarily preserved their compact identity appear red, while the most massive descendants which are dominated by other stars appear blue. In many cases, there is a color gradient of red to blue from the inner to outer regions of the galaxy indicating that the compact galaxy is concentrated at the core of its more massive descendant.

quantity) for R rather than a projected two-dimensional half-light or effective radius (which will be smaller by about 25% on average, see e.g. Hernquist 1990). This has the effect of making our values of $\Sigma_{1.5}$ smaller by ~ 0.2 dex. The threshold compactness value of 10.5 that we employ here is thus more restrictive than the cutoff of 10.3 using 2D sizes imposed by Barro et al. (2013) by ~ 0.4 dex, selecting for the very most compact galaxies in the simulation volume. (See Section 6.4 for a discussion of how our results depend on the choice of threshold.)

The descendants of these compact galaxies are traced forward in time using the merger trees described in Section 2. Figure 1 shows the properties of these descendants at $z = 2, 1, 0.5$ and 0. Satellite galaxies at each redshift are marked with triangles, and a square denotes that the compact galaxy is not in the main progenitor branch of its descendant's merger tree at that redshift, i.e. that it merged with a more massive galaxy.

Comparing the $z = 0$ and $z = 2$ panels, a couple of conclusions can immediately be drawn. First, the compact galaxies'

$z = 0$ descendants are dispersed widely among the massive galaxy population by a factor of ~ 20 in stellar mass despite having been clustered to within a factor of 3 at $z = 2$. Some galaxies maintain a similar mass all the way to the present day, while others grow by a factor of 10 or more. This order of magnitude in the spread of galaxies' descendant masses implies that rank order cannot be preserved, a topic which will be discussed in more detail by Torrey et al. (2015).

Additionally, when comparing the numbers of galaxies that fall below the $\log(\Sigma_{1.5}) > 10.5$ line, it is apparent that there are many fewer compact galaxies by $z = 0$ than there were at $z = 2$. As we will show in the following sections, processes that galaxies undergo at low redshift tend to increase their sizes as well as their masses. As a result, we predict that the comoving number density of massive, compact galaxies should decrease in the local universe (see Section 6.3).

The half-mass radius can be increased by (i) physically inflating the profile itself (i.e. shifting stellar mass to larger radii and decreasing the density everywhere) (ii) expelling mass from the inner regions, or (iii) adding mass to the outer regions. In the latter case, the half-mass radius will change while the core density remains the same, while the former two will also decrease the core density. In the middle row of panels in Figure 1, we show the stellar mass within 2 physical kpc of the galaxy center (the core mass) at the same set of snapshots. By definition, the compact galaxies sit on the high end of the distribution of core masses at $z = 2$. As time goes on, the typical core mass decreases for the compact galaxies as well as for the overall galaxy population. By $z = 0$, the compact galaxies' descendants' cores are less dense than their progenitors' by about a factor of two on average, but they are still among the densest stellar cores in the simulation. (The two obvious exceptions to this rule are massive galaxies which experienced strong interactions between $z = 0.5 - 0$ that disrupted their cores.) The evolution in core density is less pronounced than the evolution in overall size, indicating that while the first two mechanisms must be at work, the third is driving much of the total size growth.

During the 10 Gyr span between $z = 2$ and $z = 0$, many of the galaxies do experience a low level of additional star formation, and some ($\gtrsim 25\%$) even regrow a star-forming disk for some period. The amount of stellar mass formed during this time, however, is small in comparison to the mass already present in the compact bulge at $z = 2$ (typically less than 10%, though a few cases reach $20 - 30\%$). None of the galaxies ever again reach main-sequence levels of star formation. Thus, in most cases the mass growth is dominated by ex-situ stars acquired through mergers or accretion into the stellar halo. At $z = 0$, all of the compact galaxies' descendants are fully quenched with no signs of ongoing star formation. The descendants are predominantly elliptical in morphology, though a few have lenticular morphologies signifying the earlier presence of a star-forming disk.

The masses of the dark matter halos in which the galaxies are embedded are shown in the lower set of panels of Figure 1, with the stellar mass – halo mass relation appearing across the diagonal in dark pink points. The light grey points which lie above correspond to satellite galaxies. At $z = 2$, the compact galaxies are spread evenly across the scatter in the relation. At lower redshifts, the compact galaxies which still remain in the original stellar mass bin become skewed toward higher halo masses, suggesting that while the galaxies themselves are quiescent, their dark matter halos do continue to accrete and grow in mass. Similar to the stellar masses, the original factor of ~ 5 spread in halo mass at $z = 2$ has increased to a factor of 40 by $z = 0$.

One of the few quantities that does *not* experience much dispersion from $z = 2 - 0$ is the mass of the galaxies' supermassive black holes, M_{BH}. At $z = 2$, the compact galaxies host black holes with $M_{BH} = 0.6 - 3 \times 10^9$ M$_\odot$, which is overmassive by about a factor of 2.5 in comparison to the median M_{BH} in the $M_* = 1 - 3 \times 10^{11}$ M$_\odot$ range in the simulation. (As discussed in Wellons et al. 2015, the same high central gas densities which produce compact stellar distributions also feed the SMBH.) By $z = 0$, the descendants' BH masses have approximately doubled to $1 - 6 \times 10^9$ M$_\odot$, with a shallower than linear relation between the descendants' stellar and BH masses. At all descendant stellar masses, these BHs are on the high edge of the M_* - M_{BH} relation, and at lower stellar masses they become more extreme outliers. At the lowest descendant stellar masses in our study of 35 galaxies, the descendants that still lie in the same range $M_* = 1 - 3 \times 10^{11}$ M$_\odot$ host BHs with masses of $1 - 2.6 \times 10^9$ M$_\odot$, which is a factor of ~ 8 higher than the median M_{BH} in that range at $z = 0$ in the simulation. These results echo observations by Ferré-Mateu et al. (2015), who find that "über-massive" SMBHs in the local universe are hosted by massive, compact relic galaxies with old stellar populations.

4 CHARACTERIZING THE DESCENDANTS

4.1 Classifying by compact fraction

We have seen in Section 3 and Figure 1 that the compact galaxies, originally tightly grouped at $z = 2$, can accrue widely differing amounts of stellar mass by $z = 0$. What events in a galaxy's evolutionary history drive that assembly of stellar mass, and where do the stars from the compact progenitor lie within the resulting stellar distribution?

Figure 2 displays images of the $z = 0$ descendant of each of the 35 compact galaxies, ordered by decreasing descendant mass. The color in a given pixel is determined by two quantities, stellar surface density and compact fraction, as shown in the legend in the bottom right panel. The color's intensity (how light or dark it is) indicates the stellar surface density (the total mass of all the star particles along the line of sight) so that denser regions are darker. The hue is determined by the "compact fraction" (the fraction of the star particles along the line of sight which were present in the $z = 2$ compact progenitor), so that regions dominated by stars from the original compact galaxy are red and regions dominated by other stars are blue. In some cases (e.g., the rightmost two panels in the first and third rows), two compact galaxies have the same descendant. In the top row, the two galaxies were both consumed by the same massive galaxy, and in the third row the two galaxies merged together. In such cases, the two panels will then have identical surface densities but differing compact fractions, since they refer to different progenitors.

Seeing the descendants in this way again highlights the variety of experiences they undergo. Near the top where the most massive descendants reside, in many cases the compact progenitor galaxy cannot be readily identified as a single object, indicating that it was tidally shredded through an interaction with a more massive galaxy. In several of these, a band of green highlights the plane on which the compact galaxy was disrupted. In others, the core of the galaxy is orange or red while the outskirts are blue, indicating that the compact galaxy was able to maintain coherence throughout the merger process(es) and exists as the core of its descendant. Moving further down in mass, the panels which are primarily red in color are
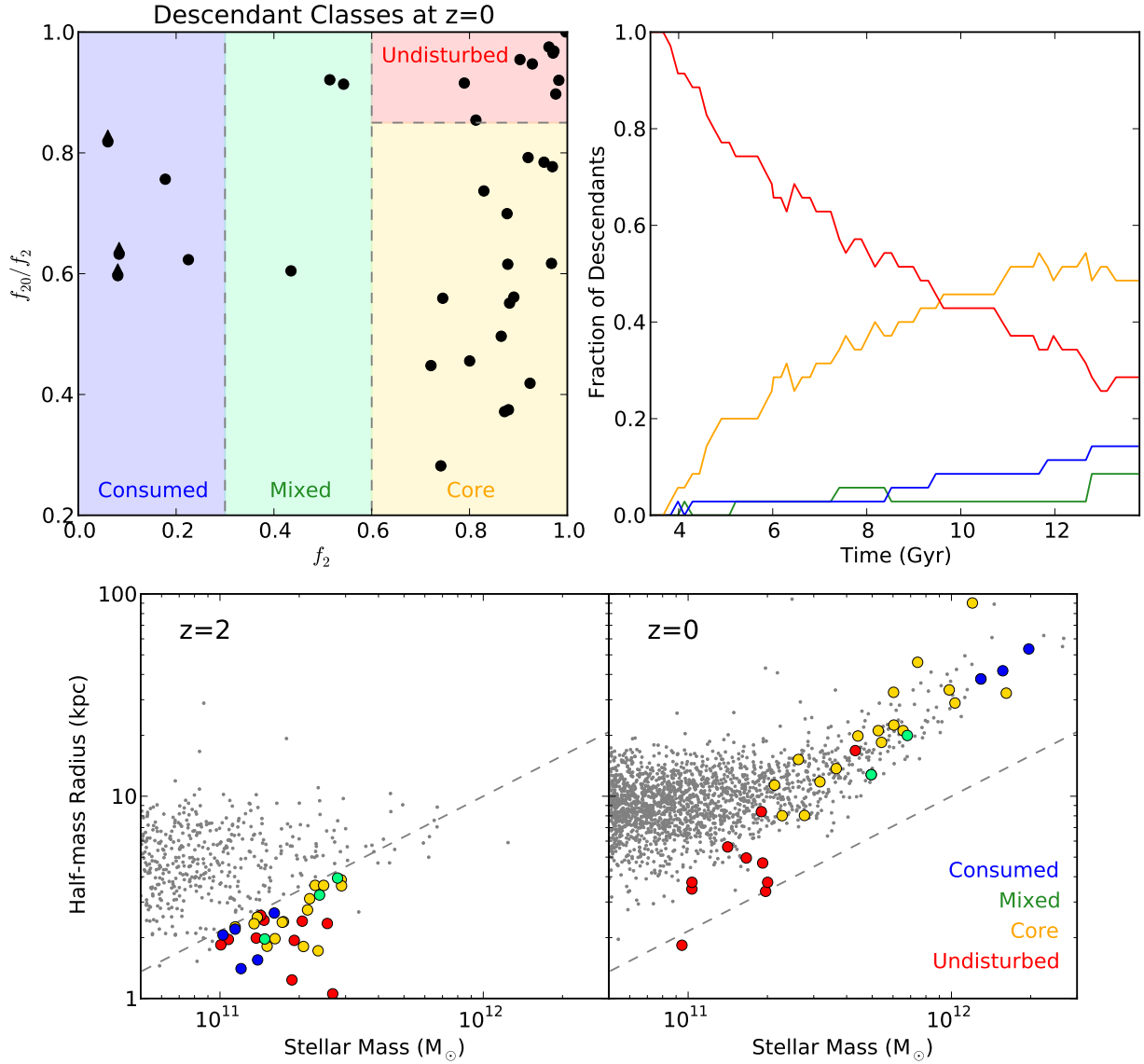
Figure 3. Classification scheme for the descendants of the compact galaxies, as described in Section 4.1, where f_r is the fraction of stars within r kpc that belong to the original $z = 2$ compact progenitor. *Top left:* Values of f_2 and f_{20}/f_2 for the final descendants at $z = 0$, with grey dashed lines and shaded regions showing how they are classified. An upward-pointing triangle indicates that $f_{20}/f_2 > 1$, so the point has been moved down by a factor of two (which does not affect the classification). *Top right:* The fraction of descendants in each class as a function of time, applying the same scheme to the descendants of the $z = 2$ compact galaxy population at each redshift. By definition, the galaxies are all initially "undisturbed" at $z = 2$, and fall into other classes as they acquire additional stellar mass. *Bottom:* The compact population at $z = 2$ *(left)* and their $z = 0$ descendants *(right)* on the size-mass plane, colored according to final descendant class. In every panel, the color blue indicates galaxies which were "consumed" by a larger galaxy, green indicates galaxies which were "mixed" in major mergers, gold indicates galaxies which are the "core" of a more massive descendant, and red indicates galaxies which survive "undisturbed" to the present day. (Note that there are fewer colored points at $z = 0$ because some of the compact galaxies have merged together.) The grey dashed line indicates our compactness criterion, $\log(\Sigma_{1.5}) > 10.5$.

compact galaxies which experienced little merger or star formation activity between $z = 2$ and $z = 0$.

To quantitatively classify this variety, we define the quantity

$$f_r = \frac{M_*(< r, \text{compact})}{M_*(< r, \text{all})} \quad (3)$$

the fraction of stellar mass interior to a radius r belonging to the compact progenitor. We then measure f_r at radii of 2 kpc and 20 kpc (chosen to be representative of the core and envelope re-

spectively) and use these quantities to inform our classification. A galaxy whose core is compact-dominated, for example, will have a high f_2. If it also has a high f_{20}, it is essentially the same galaxy, while a low f_{20} means that it has acquired an ex-situ envelope. We thus define four general classes of descendant, as depicted at $z = 0$ in the top-left panel of Figure 3:

• **Consumed:** $f_2 < 0.3$, the compact galaxy's identity was erased by accretion onto a more massive descendant.

- **Mixed:** $0.3 < f_2 < 0.6$, the compact galaxy experienced major merger activity and is partially disrupted.
- **Cores:** $f_2 > 0.6$ and $f_{20}/f_2 < 0.85$, the compact galaxy exists as the core of its more massive descendant.
- **Undisturbed:** $f_2 > 0.6$ and $f_{20}/f_2 > 0.85$, the compact galaxy has entirely preserved its identity.

The specific choice of radii as well as the dividing lines between classes are somewhat arbitrary. However, we find that the classification is not very sensitive to our specific adopted radii as long as one radius is below 3 kpc and the other is at least 8 kpc. Moreover, upon visual inspection of the mass profiles the appropriate class is obvious in nearly every case, so the boundaries can be chosen accordingly. (See Figure 4 for archetypal examples in each class and Figure A1 for the full set of profiles.) At $z = 0$, of the original 35 compact galaxies, 5 have been "consumed," 3 are "mixed," about half are "cores," and 10 are "undisturbed." The top-right panel of Figure 3 shows how the classes developed over time. All the galaxies are initially undisturbed (by definition), and over time the fraction of compact galaxies which develop outer stellar envelopes increases, leveling off at about 50%. Compact galaxies undergo mixing or consumption at a lower rate. Note that galaxies may transition between classes more than once – one galaxy, for example, is "mixed" in a major merger and then later "consumed."

The bottom panels in Figure 3 show again the compact galaxies at $z = 2$ and their descendants at $z = 0$ on the mass-radius plane, this time colored according to the class to which the descendant belongs. At the low-mass end at $z = 0$, the descendants all belong to the "undisturbed" class in red, since they have gained very little stellar mass. At the high-mass end, those descendants which have consumed a compact galaxy are shown in blue. Between those extremes lie compact galaxies which are cores (in orange) and which were thoroughly mixed by merging (in green). (Note that there is not always a one-to-one correspondence between $z = 2$ and 0 because some of the compact galaxies have the same descendant.) Examples showing the evolution of an individual galaxy from each of these classes are shown in Figure 4 and discussed in the following subsection.

4.2 Representative evolutionary examples

Each of the four sets of panels in Figure 4 is composed of three items demonstrating how a single compact galaxy from $z = 2$ developed the characteristics that determined its descendant group at $z = 0$. The bottom left panel in each frame shows the evolution in stellar mass, with major mergers marked with a vertical dotted grey line and the stellar mass ratio listed at the top of the panel. Large grey points correspond to the six images above, which are colored using the same scheme as in Figure 2 where a color's intensity indicates stellar surface density and hue indicates the fraction of stars belonging to the compact progenitor. The image farthest to the left depicts the compact progenitor at $z = 2$, and the image farthest to the right depicts its final $z = 0$ descendant. The cumulative stellar mass profile of this descendant is plotted in the panel in the lower right of each frame with a black line. The red line, for contrast, shows the cumulative stellar mass profile of only those stars belonging to the compact progenitor. The ratio of the red to black line is the quantity f_r described in Section 4.1. Grey dashed lines mark the locations of f_2 and f_{20} which were used to classify the descendants. Each of these examples demonstrates the kind of event (or lack thereof) that determines the final descendant type, and is representative of that class.

4.2.1 Consumed

In the first (blue) frame in Figure 4, the mass evolution shows a sudden jump around 9 Gyr which marks the point in time when the compact galaxy merges into a much more massive galaxy. As it is falling in, its outer stellar envelope is slowly stripped away before the core finally falls into the central object. The images above show that the compact galaxy is completely torn apart and its identity erased, though it is still faintly visible at $z = 0$ as a band of green tracing the orbital plane along which it was disrupted. Five of the 35 compact galaxies (14%) fall into this class at $z = 0$. Their $z = 2$ progenitors tend to fall into the lower-mass end of the selection range, which is not surprising since the less massive a galaxy is, the more likely that a merger partner will be capable of disrupting it. Interestingly (and perhaps unexpectedly), the regrowth of a star-forming disk is visible in the second image of the sequence. This is not an uncommon event among the objects in our sample, with disk regrowth occuring at some point for about a quarter of them. These disks are very minor in terms of their stellar mass when compared to the mass of the core, but would undoubtedly make up a more significant portion of the light during their star-forming period.

4.2.2 Mixed

The second (green) frame shows a galaxy which was primarily undisturbed until about 12 Gyr. At that time, it experienced a merger with another galaxy of similar mass. As the two galaxies spiraled in together, their stars became thoroughly mixed. As is visible in the profiles on the right, stellar material from the compact progenitor is distributed uniformly throughout the final descendant and makes up a large fraction of its total mass. Only 3 of the 35 compact galaxies (9%) fall into this class, as mergers between galaxies of nearly the same mass and binding energy are rare.

4.2.3 Cores

An example of the third and most common type of descendant is shown in the third (orange) frame. This galaxy experienced two major mergers between $z = 2$ and 0, along with several more minor mergers. At 6 Gyr, it disrupts another galaxy of 75% its mass and gains a thin stellar envelope. Later, around 11 Gyr, it does the same to another loosely bound massive galaxy at a similar mass ratio, ultimately residing at the core of a final descendant many times its original mass.

These 3:4 merger events are not so different in terms of stellar mass ratio from the 1:1 merger in the previous (mixed) case. The crucial difference between the two cases is not necessarily mass, but gravitational binding energy. In dissipationless mergers, it has been shown that particles tend to preserve their rank order in binding energy, with the most tightly bound particles of the merger progenitors remaining the most tightly bound particles of the descendant (Barnes 1988; Hopkins et al. 2009b). The compact galaxies, with their large masses and small sizes, are very tightly bound. Thus, they are more likely to survive a merger intact even in cases of near unity mass ratios, and it requires a galaxy of similar or greater mass to unbind these objects (as in the previous two examples). 17 of the original 35 compact galaxies (49%) survive as the cores of more massive descendants in this manner.
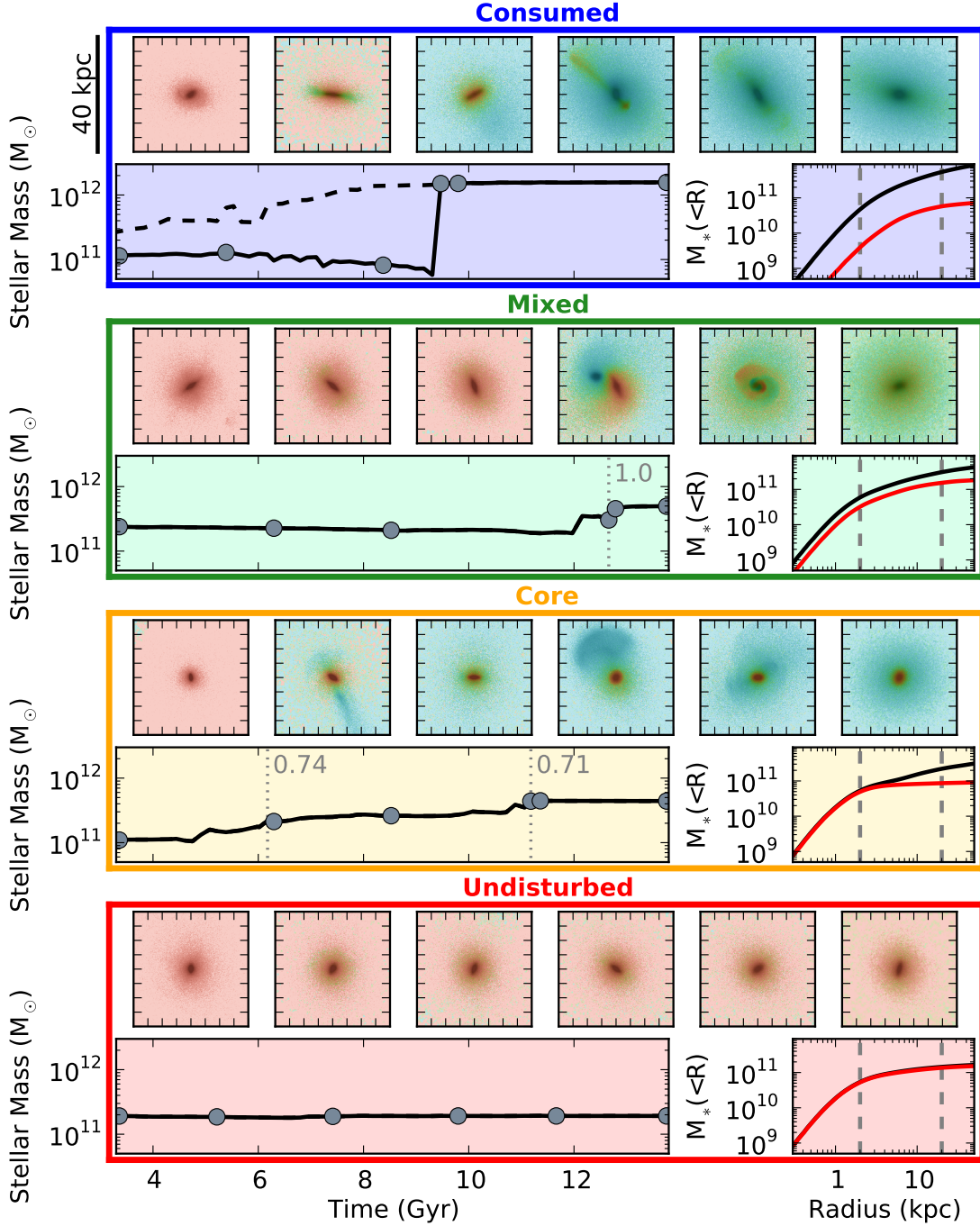
Figure 4. Evolution of an individual galaxy from each of the four descendant types. For each of these examples, the panel on the left shows the evolution of stellar mass with time in a solid black line, with dashed lines drawn for merger partners where applicable. Large grey points mark the times corresponding to the six images directly above, which have the same color scheme as in Figure 2. The rightmost panels show the cumulative stellar mass profiles for the final $z = 0$ descendants. Black lines include all stellar mass, while the red lines only include star particles that were present in the compact progenitor at $z = 2$. The ratio of these two lines is the f_r discussed in Section 4.1 used to classify the descendants, and grey dashed lines show where f_2 and f_{20} were measured. Each of these examples is demonstrative of the kind of events (or lack thereof) that characterize each descendant type.

4.2.4   Undisturbed

The evolution of the final object (red frame) is remarkable in its un-eventfulness. This galaxy maintains the same stellar mass throughout its evolution, gaining stars neither through accretion, mergers, nor in-situ star formation. Ten objects from our sample of 35 (29%) are similarly able to avoid further action and thus completely main-

tain their same identity from $z = 2$ (though not all are quite so pristine). Though these galaxies do not grow in stellar mass, they do grow in size, a topic which is further discussed in Section 6.2.
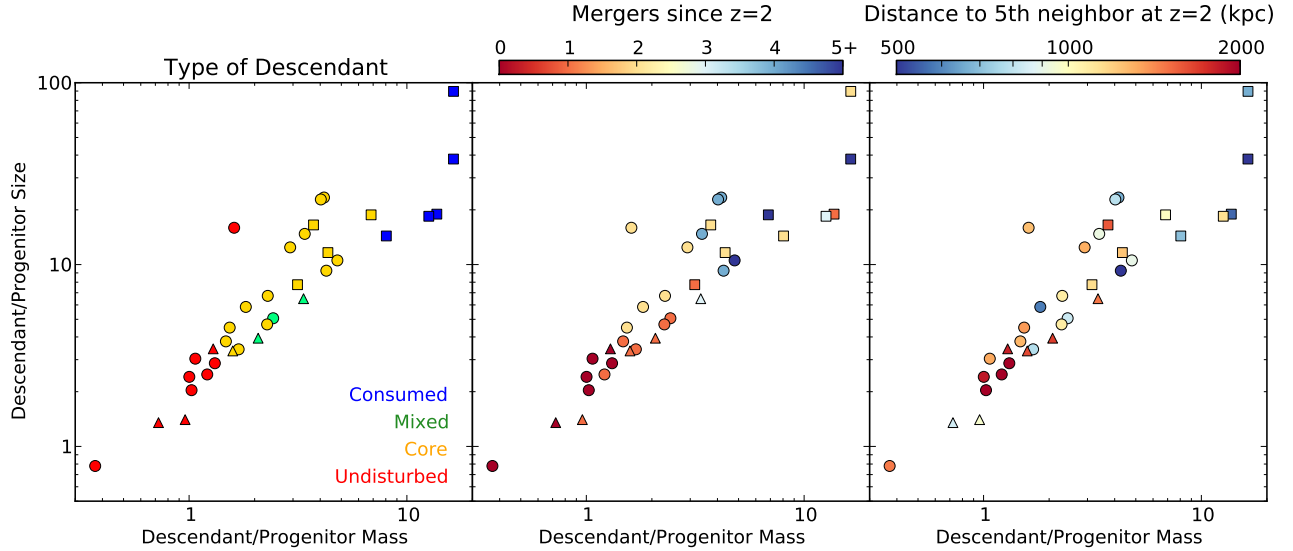
Figure 5. Growth in size and mass among the compact galaxy population from $z = 2 - 0$. In all three panels, the x-axis shows the mass growth (ratio of a galaxy's stellar mass at $z = 0$ and $z = 2$) and the y-axis shows the size growth (ratio of the stellar half-mass radii). As in Figure 1, triangles indicate that a galaxy is a satellite at $z = 0$ and squares indicate that the compact galaxy does nie lie along the main progenitor branch of its descendant. *Left panel:* color refers to the type of descendant, as defined in Section 4.1. *Middle panel:* color indicates the number of mergers since $z = 2$ with stellar mass ratios of $<10:1$. *Left panel:* color indicates $z = 2$ environment, i.e. the distance to the 5th nearest neighbor with an r-band magnitude of at least -19.5 (about 10^9 M$_\odot$). The most isolated galaxies (red on the rightmost panel) tend to experience fewer mergers (red on the middle panel) and thus experience little mass growth and are essentially undisturbed. Two notable exceptions are satellite galaxies, which fell into another DM halo in the intervening time period but have not merged with the central galaxy.

5 ENVIRONMENT

What determines which of these evolutionary paths a galaxy will take? Clearly, mergers are a very important component of their growth. The compact galaxies are primarily quiescent at $z = 2$ and retain low specific star formation rates throughout their lifetimes, so most of their mass growth is due to the acquisition of ex-situ stars through mergers and interactions. Figure 5 shows the relative growth in both mass (x-axis) and size (y-axis) for the compact sample between $z = 2$ and 0. In the first panel, galaxies are colored according to their descendant type, as in Figure 3. The bottom left region of this panel is dominated by the undisturbed (red) compact galaxies which have experienced little size and mass growth, while the rightmost galaxies are those which were consumed (blue) by their very massive descendants.

In the middle panel, the symbol color indicates the number of mergers with stellar mass ratios of at least 1:10 that the galaxies have experienced since $z = 2$. The gradient in color from red to blue with increasing mass growth shows that, as expected, the more merger activity a galaxy experiences, the more stellar mass it gains and the more likely it is to fall into the "core" or "consumed" groups.

In turn, a galaxy's merger rate is a function of its environment. For this subsample of galaxies, it appears that in denser, more crowded environments, the galaxies are more likely to merge with their neighbors of comparable mass. The rightmost panel of Fig. 5 demonstrates this correlation by coloring the same points according to the compact progenitors' $z = 2$ environments, quantified as the distance to the 5th nearest neighbor with an r-band magnitude of at least -19.5 (corresponding to a stellar mass of about 10^9 M$_\odot$) as in Vogelsberger et al. (2014a). The same trend appears in this panel as in the middle one, indicating that a galaxy's environment has some power to predict how it will evolve. The more isolated (red) a com-

pact galaxy is, the fewer mergers it will undergo, and the less mass growth it will experience. The descendants of the galaxies which were in isolation at $z = 2$ and experienced little merger activity in the interim are also preferentially isolated at $z = 0$. The connection between galaxy merger rate and environment will be explored in more detail for all Illustris galaxies by Rodriguez-Gomez et al. (in prep).

Two interesting exceptions to the merger rate/environment correlation are the white triangles in the lower left corner, which were in moderately dense environments at $z = 2$ but experienced very little mass growth. At $z = 0$, these two are satellite galaxies which have fallen into a nearby massive dark matter halo in the intervening 10 Gyr but have not (yet) merged with the central galaxy. A similar DM-only result is reported by Stringer et al. (2015), who find that the most compact DM structures in the simulation are substructures embedded in larger halos. Based on this evidence, we predict that massive compact relics in the local universe should preferentially live in regions where they are protected from mergers, either in isolation or as satellites in a larger group. The latter option also has some observational support from Valentinuzzi et al. (2010), who have found that nearby massive compact galaxies tend to live in cluster environments.

6 DISCUSSION

6.1 Compact galaxies as cores

Given that about half of the compact galaxies from $z = 2$ exist at $z = 0$ as the cores of very massive galaxies, one can ask the reverse question: how many massive galaxies have cores which were once compact galaxies? We address this question by tracing all the $z = 0$ massive galaxies through the merger tree and calculating $\Sigma_{1.5}$ at each point on its main progenitor branch. We then define the
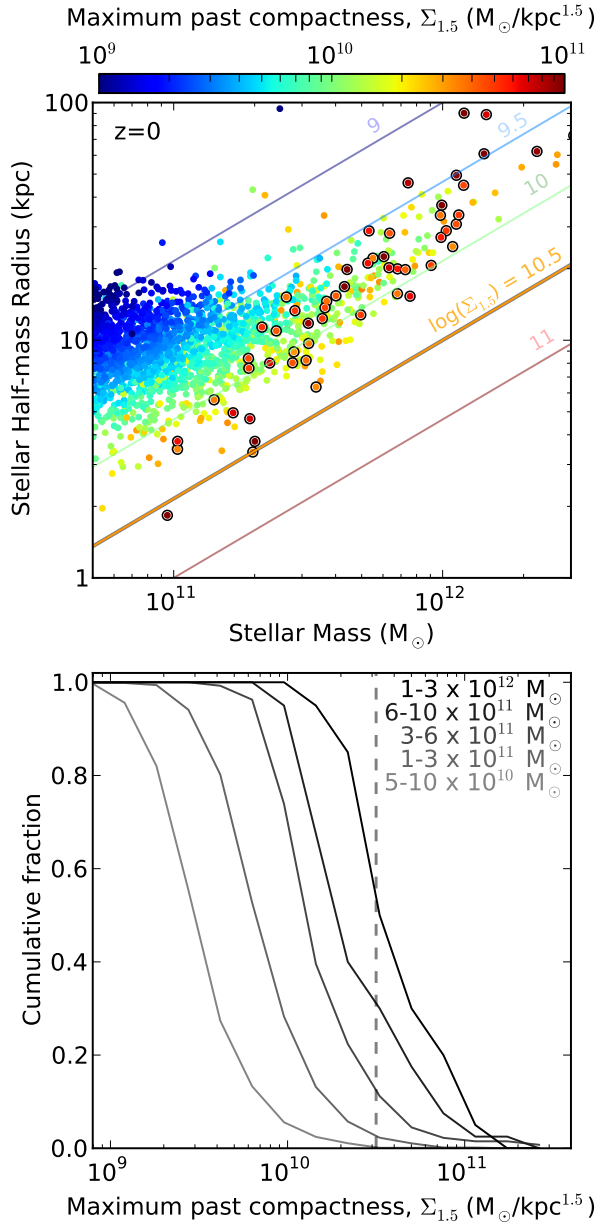
Figure 6. *Upper panel:* Mass-size plane at $z = 0$ for Illustris galaxies. Color indicates the maximum compactness ($\Sigma_{1.5}$) of all the galaxy's progenitors along the main branch of its merger tree above 10^{10} M$_\odot$. Solid colored lines mark a constant value of $\Sigma_{1.5}$. Galaxies which have satisfied $\log(\Sigma_{max}) > 10.5$ (the compactness criterion employed in this paper) *at any redshift* are marked with black circles. (Over half of these are the same 35 which were compact at precisely $z = 2$.) *Lower panel:* Cumulative distribution of Σ_{max} for all galaxies, binned by stellar mass and normalized against the number of galaxies in each bin. Thus, given a value of $\Sigma_{1.5}$ (e.g. $10^{10.5}$, marked with a vertical dashed line), one can determine what fraction of galaxies at a given stellar mass have ever achieved that level of compactness. There is a clear relationship between stellar mass and compactness – more massive galaxies have more compact progenitors – but the trend has significant dispersion.

"maximum past compactness" Σ_{max} to be the maximum value[1] of $\Sigma_{1.5}$ when the progenitor had a stellar mass of at least 10^{10} M$_\odot$. In contrast to the analysis thus far, this approach permits a galaxy to be compact at any redshift, rather than specifically tying them to $z = 2$. This allows, for example, a galaxy which forms very early at $z = 3-4$ in a compact state but grows out of the compact population by $z = 2$, or a galaxy which forms via a compact starburst at $z = 1.5$, both of which would be missed by the preceding analysis.

The colors of the points on the mass-size plane in the upper panel of Figure 6 indicate Σ_{max} for all of the massive galaxies at $z = 0$. Lines of constant $\Sigma_{1.5}$ are drawn in the same color scheme. Any galaxy whose primary progenitor met the $\log(\Sigma_{1.5}) > 10.5$ compactness criterion at any point in time is outlined in black. About half of these were compact at exactly $z = 2$ and overlap with the sample discussed elsewhere in this paper, while the other half experienced their compact phases at other redshifts. From this scatter plot, there is a clear trend between mass and maximum past compactness: more massive galaxies tend to have more compact progenitors. (See also Genel et al. (2014) for a discussion of the relationship between mass and compactness in Illustris.) Thus, many of the most massive galaxies were indeed once compact galaxies according to our definition – but it is interesting to note that this is not universally the case, since there is also considerable scatter in the distribution of Σ_{max} at this mass (and, in fact, at all masses).

The relationship between mass and Σ_{max} is further quantified in the lower panel of Figure 6. Each line shows the cumulative fractional distribution of Σ_{max} for the galaxies in a given stellar mass bin. As was suggested by the upper panel, moving to lower masses shifts the distribution to lower compactness values. For any $\Sigma_{1.5}$, we can now see what fraction of galaxies at that mass have ever met that threshold. The orange line denotes the $\log(\Sigma_{1.5}) > 10.5$ criterion used elsewhere in this paper. Approximately 55% of galaxies with $M_* > 10^{12}$ M$_\odot$ have met this definition of "compact," along with 30% of 6-10 $\times 10^{11}$ M$_\odot$ galaxies, 15% of 3-6 $\times 10^{11}$ M$_\odot$ galaxies, etc.

Although a substantial fraction (55%) of very massive galaxies are former compact galaxies, it is important to note that few of these were compact at exactly $z = 2$. Rather, their compact phases are spread over $z = 1-3$, so that only about 15% of galaxies above 10^{12} M$_\odot$ at $z = 0$ have compact progenitors at $z = 2$. Similarly, of the 35 $z = 2$ compact galaxies, only 3 (9%) have direct descendants in that mass range at $z = 0$. These fractions demonstrate once again that while there is indeed a strong trend between final stellar mass and past compactness, there is also a large dispersion in galaxies' evolutionary tracks that cannot be neglected.

6.2   Mechanisms for size growth

Nearly all of the compact galaxies have grown in size as well as mass since $z = 2$, with very few still remaining in the compact regime at $z = 0$. Potential origins of this growth include physical effects such as major mergers (Hernquist, Spergel & Heyl 1993; Hopkins et al. 2009b), minor mergers and accretion (Naab, Johansson & Ostriker 2009; Hopkins et al. 2010), star formation (Graham, Dullo & Savorgnan 2015), and adiabatic expansion due to the expulsion of gas from the galaxy through stellar winds and BH feed-

---

[1] Occasionally, SUBFIND or the merger tree will misassign ownership of star particles or DM halos for a single snapshot, throwing off the calculated mass or size. To minimize the effect of these glitches, we actually use the second-highest $\Sigma_{1.5}$.
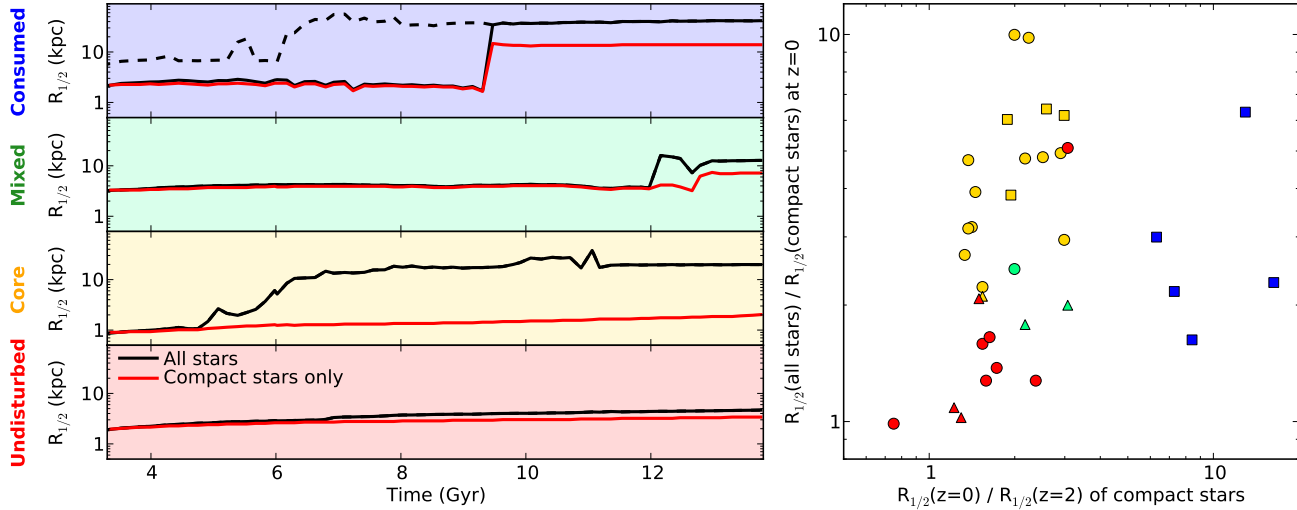
Figure 7. Compact galaxies' size evolution from $z = 2 - 0$. *Left panels:* Size evolution of the same four galaxies shown in Fig. 4, one from each descendant group. Black lines track the half-mass radius of the descendants' entire stellar distribution, while the red lines track the half-mass radius of only those stars which were part of the $z = 2$ compact progenitor. In the "consumed" and "mixed" cases, disruptive mergers increase the compact half-mass radius along with the overall half-mass radius. In the "core" case the compact galaxy remains essentially same size while the overall half-mass radius increases due to a buildup of additional stellar mass at larger radii, and in the "undisturbed" case the compact galaxy changes very little, having accreted or formed a very small amount of stellar mass since $z = 2$. *Right panel:* For each of the descendants of the 35 compact galaxies, *x-axis:* Growth in half-mass radius of the compact progenitor's stars, i.e. the ratio between the value of the red line at $z = 0$ and $z = 2$. *y-axis:* Half-mass radius of all stars relative to the half-mass radius of compact stars, i.e. the ratio between the black and red lines at $z = 0$. Higher values in the x-direction indicate disruption of the compact core, while higher values in the y-direction indicate the presence of ex-situ stars at large radii. Symbol shapes and colors are the same as in Figs. 3 and 5.

back (Fan et al. 2008, 2010), as well as numerical effects stemming from the non-constant physical size of the gravitational softening length in Illustris.

To examine the importance of each of these mechanisms for the size growth of the different descendant types, let us return to the same four example galaxies we discussed in Section 4.2. The left-hand panels of Figure 7 show the evolution of their stellar half-mass radii with time. In addition to the black line for total stellar half-mass radius (which includes all stars bound to the object), we also show a red line for the the "compact half-mass radius" – that is, the half-mass radius including only those stars which belonged to the compact progenitor at $z = 2$. This allows us to disentangle the growth of the compact core from the growth of the galaxy as a whole.

In the first (consumed) case, both the overall and compact half-mass radii jump up when the compact galaxy falls into the more massive central galaxy. This indicates, as we have seen, that the compact galaxy's stellar mass has been dispersed throughout the descendant. In a similar (though less extreme) way, the second (mixed) galaxy's compact half-mass radius increases abruptly when it undergoes a disruptive major merger[2]. In these cases, the size growth is primarily driven by merging.

Conversely, in the third (core) case the compact half-mass radius hardly changes despite plenty of mergers and stellar mass growth, while the total half-mass radius greatly increases. The very small change in compact half-mass radius signifies that the core has remained intact, and that the vast majority of the overall size growth

is driven by the acquisition of outer layers of stellar material from less-bound galaxies.

Finally, the galaxy which is undisturbed grows only slightly in size from 2 to 3 kpc over this 10 Gyr period. In this case, because there is little to no mass growth, the only two mechanisms remaining to explain the size growth are adiabatic expansion from mass loss, and numerical effects. In treating the gravitational forces between baryons, Illustris uses a gravitational softening length ϵ_b which is a fixed comoving size at redshifts $z \geq 1$. The increase of the physical scale on which the potential is softened will decrease the depth of the gravitational well in dense regions, artificially inflating the stellar mass profiles as the star particles become less gravitationally bound. It is unlikely that the increasing ϵ_b is the sole culprit, however, since it is capped at a fixed physical size at $z = 1$ but the size growth does not completely halt at this time. Moreover, numerical "relaxation" of the galaxies' $z = 2$ profiles to the $z = 0$ softening length shows that this effect alone should only change the half-mass radius by about 15% (see Appendix A). Thus, we expect that the remaining 35% of the growth stems from physical effects, e.g. expansion as a response to mass loss from stellar winds and AGN feedback, or residual star formation at larger radii.

Returning to the compact population as a whole, the right-hand panel of Figure 7 shows the growth in compact half-mass radius since $z = 2$ (x-axis) against the ratio between the overall and compact half-mass radii (y-axis) for each $z = 0$ descendant. The x-axis quantity is identical to the ratio between the value of the red lines in the left-hand panel at $z = 0$ and $z = 2$, while the y-axis quantity is the ratio between the black and red lines at $z = 0$. A high x-value here indicates some disruption of the compact core, like the mergers that caused jumps in the compact half-mass radius in the first and second examples on the left. All of the "consumed" galaxies, whose stellar contents have been scattered far and wide, are therefore located on the far right of this panel. A high y-value indicates

---

[2] The increase in total half-mass radius slightly ahead of the increase in compact half-mass radius marks the moment when SUBFIND assigned the merger partner's outer stellar layers to the compact galaxy, prior to the actual merger event.

the presence of significant ex-situ stellar mass at large radii, so that the "core"-type descendants separate from the "undisturbed" descendants despite having similar x-values in many cases. In general, the growth in compact half-mass radius is much smaller than that of the overall half-mass radius. This implies that a majority of the size growth is due to the addition of stellar mass in the outer parts of the galaxies. Galaxies which gained little stellar mass typically grow by about 50% or less in compact half-mass radius, while those which experienced some merger events are slightly more perturbed, and those which experienced majorly disruptive mergers grow even more.

6.3   Implications for the number density of compact galaxies

As we have seen in the previous subsection, nearly all of the compact galaxies grow in size between $z = 2$ and $z = 0$ even if they experience little growth in mass. Of the original 35 compact galaxies, only two remain below the compactness threshold at $z = 0$. Shifting the threshold up slightly to account for the 15% change in half-mass radius from numerical effects yields one additional galaxy, for a final "survival fraction" of 9% for compact galaxies from $z = 2$ to the present day. (And of these three, one is an extreme case which dives through a massive halo, is stripped of its stellar envelope along the way, and is just escaping out the other side at $z = 0$, having managed to *decrease* in both size and mass!)

The number density of compact galaxies depends not only on the rate at which galaxies *leave* the compact population, but also the rate at which they *enter*. Our previous study (Wellons et al. 2015) found mechanisms for producing compact galaxies which are most efficient in the high-redshift universe when cold, dense gas is abundant. As time increases and the universe becomes more rarefied, we expect that the production rate of compact galaxies should also decrease. In Section 6.1, we identified all the galaxies in the simulation which had a massive ($< 10^{10}$ M$_\odot$), compact progenitor at any redshift. For each of these galaxies, we have measured the median redshift of the compact phase as well as its total duration. The median redshifts of the compact phases are broadly distributed from $z = 1 - 3$, falling off at higher and lower z and implying that the compact formation mechanisms indeed no longer operate as efficiently at low redshift. Half of the compact phases lasted less than 2 Gyr, and only 10% were longer than 5 Gyr, indicating that we should expect few massive, compact galaxies to remain in the local universe.

Both of these exercises (choosing compact galaxies at $z = 2$ and tracing them forward, and finding "ex-compact" galaxies at $z = 0$ and examining the time and duration of their compact phases) indicate that the number density of massive, compact galaxies should decrease at low redshift. Physically, this is a reflection of the growing dominance of dissipationless processes (e.g. dry mergers) at late times over processes such as disk instability or wet mergers, more common at high redshift, which provide a way to dissipate angular momentum and thus produce more compact stellar populations.

6.4   Contextualizing the results

Studies of compact massive high-redshift galaxies adopt varying initial selection methods, including differences in the compactness criterion (e.g. the slope and normalization of the power-law cut across the mass-radius plane), minimum stellar mass, quiescence (e.g. cuts in sSFR, UVJ, or morphology), size estimation (e.g. major-axis vs. circularized half-light radius, bulge-disk decomposition vs. single-Sersic fits), and parent surveys (e.g. SDSS, CANDELS, COSMOS). These differences can make direct comparisons between observational surveys that infer the the mass or size evolution of massive compact galaxies difficult. In this paper, we have primarily focused on the *physical* mass and size evolution of compact massive galaxies as realized in a cosmological simulation, which introduces an additional level of complexity when making comparisons. In this subsection, we discuss some of the specific definitions used in this paper and their impact on our conclusions, which may help the reader to place these results in the context of other work, particularly observational work.

One question which plagues both simulators and observers is, what is the most meaningful way to talk about size? In this paper we have opted to use the stellar half-mass radius – unambiguously defined as "the radius of the sphere containing half of the stellar mass which is gravitationally bound to this object" – as our fiducial measurement of size. Using the stellar half-mass radius as a proxy for galaxy size has the disadvantages that it is not a directly observable quantity, and that it can be perturbed by the addition of stellar mass at some larger radius when the density profile is steep. However, the half-mass radius has clear physical meaning, can be easily and robustly calculated directly from SUBFIND data, and is related to the circularized half-light radius (modulo variations in the mass-to-light ratios for differently-aged stellar populations). In principle we could have adopted galaxy size estimates by fitting profiles to the stellar light distributions of every galaxy in the simulation and measuring an effective or scale radius (e.g., as done in Wellons et al. 2015). However, given the complexity and variety of the simulation data the resulting radii would likely be sensitive to several details of the fitting procedure and would likely not yield characteristically different trends from those found and presented in this paper. Nevertheless, it could be worthwhile to consider in the future a more even-handed comparison of galaxy size evolution for compact massive galaxies.

Another choice we have made in the above analysis is a particular selection of compactness threshold value, $\log(\Sigma_{1.5}) > 10.5$. We mentioned in Section 3 that this selection is more severe than that employed by e.g. Barro et al. (2013). How sensitive are the results to this particular choice of "compactness"? To explore this question, we repeated the analysis with a more comparable threshold of $\log(\Sigma_{1.5}) > 10.1$, which yielded a sample of 103 galaxies in the same $1 - 3 \times 10^{11}$ M$_\odot$ mass range. These galaxies are more likely to be star-forming than the original sample of 35 (only 42% of them have specific star formation rates lower than 3×10^{-10}/yr, as opposed to 66% in the original sample), so more of them quickly leave the compact regime due to star formation at large radii. When this population is traced forward, we find that they are more likely than the original sample to have descendants in the "mixed" or "consumed" groups, since they are larger (less tightly bound) and hence easier to disrupt via merger. Overall, however, we find that the same trends hold as have been described above, and therefore it seems that the qualitative conclusions drawn about the diversity of growth paths for massive compact galaxies is not highly sensitive to how they are initially selected.

A more implicit set of assumptions adopted in this paper is the physical/feedback model employed by the Illustris simulation. The masses and sizes of the simulated galaxy populations examined in this paper are specifically subject to influence from the finite mass resolution and spatial softening, pressurization of the ISM, and AGN feedback model. We discuss in some detail the potential effects of gravitational softening (and its redshift evolution) in

the Appendix of this paper. The gravitational softening and ISM pressurization adopted in this paper can potentially prevent galaxies from fully collapsing during dissipational events such as gas-rich galaxy mergers. In general, both gravitational softening and our method of ISM pressurization risk overestimating the sizes of galaxies and it is therefore possible that some galaxies that would at one time be compact would be missed. Thus, our conclusions about the fractions of galaxies which pass through a compact phase might best be viewed as a lower limit. However, the basic convergence study presented in Wellons et al. (2015) indicated that the sizes of galaxies are well-converged at the $z = 2$ gravitational softening level, so the results should not dramatically change. Our ability to further investigate the impact of these simulation traits on our results is limited since we cannot easily re-run the Illustris simulation volume. Reconsidering the conclusions presented in this paper with other simulations (e.g. EAGLE, Schaye et al. 2015; Crain et al. 2015) or with zoom-in re-simulations of the specific objects studied in this paper or objects selected from other large full-volume simulations may provide additional context for these results in the future.

Finally, we would like to emphasize that the results herein are primarily focused on very massive galaxies with stellar masses of at least 10^{11} M$_\odot$ at $z = 2$, and that caution is warranted when comparing to results in other mass regimes where different physical processes may govern the evolution.

7   SUMMARY AND CONCLUSIONS

Herein, we have identified a population of 35 massive $(1 - 3 \times 10^{11}$ M$_\odot)$ galaxies at $z = 2$ in the cosmological hydrodynamical simulation Illustris which satisfy the compactness criterion $\log(\Sigma_{1.5}) > 10.5$. We have traced these massive, compact galaxies forward in time through the simulation to their $z = 0$ descendants at the present day. Our most important findings are summarized below:

• Though the compact galaxies all originated at $z = 2$ with the same stellar mass to within a factor of 3, by $z = 0$ their stellar masses differ up to a factor of 20. Similarly, their DM halo masses, originally within a factor of 5, spread to a factor of 40. Rather than remaining tightly grouped, the descendants' stellar masses are dispersed throughout the entire massive galaxy population at $z = 0$.

• The compact galaxies can undertake a variety of evolutionary paths to $z = 0$. Approximately half survive as the core of a more massive descendant, about 15% are consumed and destroyed in a merger with a much more massive galaxy, about 30% are generally undisturbed by mergers, accretion, or star formation activity, and the remaining few are thoroughly mixed by major mergers. These percentages are a weak function of initial stellar mass, with less massive galaxies more likely to be consumed and more massive galaxies more likely to be cores.

• Very few (about 10%) of the galaxies from the $z = 2$ compact sample still satisfy our compactness criterion at $z = 0$, suggesting a decrease in the number density of massive, compact galaxies at low redshift in the absence of any replenishing compact formation mechanism.

• A compact galaxy's $z = 2$ environment has some predictive power for its final evolutionary outcome. Compact galaxies in denser environments (with the exception of satellite galaxies) are more likely to undergo mergers and gain stellar mass at larger radii, losing their compact identity in the process. Those which are isolated at $z = 2$ and experience little merger activity are also preferentially isolated at $z = 0$. Thus we predict that massive, compact

relics in the local universe should predominantly live in underdense environments or as satellites in larger groups.

• A galaxy's $z = 0$ stellar mass is related to the compactness of its progenitors, such that more massive galaxies are more likely to have once been compact. However, this trend possesses significant dispersion and it is *not* the case that the most massive galaxies at $z = 0$ can be directly linked to massive compact galaxies at $z = 2$. While more than half the galaxies with stellar mass $> 10^{12}$ M$_\odot$ at $z = 0$ have a direct compact progenitor at some redshift, only 15% have a compact progenitor at exactly $z = 2$.

• The dominant source of size growth for the compact galaxies is the addition of ex-situ stellar mass at larger radii through mergers and accretion into the stellar halo, followed by disruptive major mergers, with smaller contributions from ongoing or renewed star formation, adiabatic expansion due to mass loss, and/or numerical effects.

APPENDIX A: "ADIABATIC EXPANSION" FROM A CHANGING GRAVITATIONAL SOFTENING LENGTH

To estimate the effect of a changing gravitational softening length ϵ on the matter distributions of galaxies which are undisturbed between $z = 2 - 0$, we mimic the process of adiabatic expansion that is invoked as a response to mass loss from the center of the potential on timescales longer than a dynamical time, $\tau_{\rm ej} > \tau_{\rm dyn}$. Expansion occurs in such a way as to conserve particles' specific angular momentum $r v(r)$, which is an adiabatic invariant. If the distribution is spherically symmetric and particles move on circular orbits, $r \propto M(< r)^{-1}$. Changing the gravitational softening length will have much the same effect – not by physically removing mass, but by changing how much of it an external particle "feels." Given a distribution of mass $\rho(r)$ and the scale ϵ on which gravity is softened, we can define an "effective mass enclosed" $M_{\rm eff}(r, \epsilon)$ which decreases with increasing ϵ.

Consider the case where gravitational forces are Plummer-softened, so that the gravitational force per unit mass dF exerted by a parcel of mass dm on a test particle is

$$dF = \frac{G\, dm\, r_g}{(r_g^2 + \epsilon^2)^{3/2}}$$

where r_g is the distance between the mass and the test particle, and ϵ is the gravitational softening length. (Illustris employs a slightly different spline potential (see Hernquist & Katz (1989); Springel (2010)) but the Plummer potential is much more analytically pliable and is similar enough for our purposes here.) If the test particle lies at a distance R from a spherically-symmetric distribution

of mass with density profile $\rho(r)$, we can integrate over a series of concentric shells in r to determine the total gravitational force. Each shell consists of a series of rings around the line connecting the test particle and the center, so that on a given ring (described by the angle θ from the connecting line), all points are the same distance r_g from the test particle and the same distance r from the center and hence exert the same force $dF \cos \phi$ along the connecting line. By the law of cosines

$$r_g^2 = r^2 + R^2 - 2rR \cos \theta$$

and by the law of sines

$$\cos \phi = \sqrt{1 - \left(\frac{r}{r_g}\right)^2 \sin^2 \theta}$$

so that the gravitational force integrated over the entire sphere interior to R is

$$F_r = \int_0^R \int_0^\pi \frac{G\rho(r)2\pi r^2 \sin\theta \, r_g}{(r_g^2 + \epsilon^2)^{3/2}} \frac{(R - r\cos\theta)}{\sqrt{r^2 + R^2 - 2rR\cos\theta}} d\theta dr$$

The integral over θ has an analytical solution

$$
\begin{aligned}
F_r &= \int_0^R \frac{G\rho(r)4\pi r^2}{R^2} \left[\frac{1 + \epsilon^2/r^2 + R/r}{2\sqrt{\epsilon^2/r^2 + (R/r + 1)^2}} \right. \\
&\quad \left. - \frac{1 + \epsilon^2/r^2 - R/r}{2\sqrt{\epsilon^2/r^2 + (R/r - 1)^2}} \right] dr \\
&\equiv \frac{G}{R^2} \int_0^R 4\pi r^2 \rho(r) \beta(r, R, \epsilon) dr \\
&\equiv \frac{GM_{\text{eff}}(R, \epsilon)}{R^2}
\end{aligned}
$$

where the "density correction function" $\beta(r, R, \epsilon)$ is the ratio between the actual mass *present* in a shell at radius r and the mass *felt* by a test particle at R if gravity is Plummer-softened on scales of ϵ.

The form of $M_{\text{eff}}(R, \epsilon)$ will vary with the density profile $\rho(r)$ and is in general not analytically solvable, so it must be evaluated numerically. We can directly apply the above to any arbitrary mass profile, including those we recover from the simulation. In practice, we would like to answer the following question: If a galaxy has a stellar mass profile $\rho(r)$ when the softening length is ϵ_1, what will it be after the softening length is (slowly) changed to ϵ_2?

To relax the profile to a new softening length, we first measure the adiabatic invariant $rM_{\text{eff}}(r, \epsilon_1)$ at shells of r_i in the initial profile, as well as recording the masses $m_{i-1/2}$ between the shells. We then change the softening length to ϵ_2, remeasure $r_i M_{\text{eff}}(r_i, \epsilon_2)$ and compare it against the original value. Starting with the innermost shell, we iteratively change r_i until the adiabatic invariant is within some error tolerance of its initial value (placing $m_{i-1/2}$ halfway between the shells' new locations), then move on to the next shell and work our way out.

The results of performing this exercise on the compact galaxies' $z = 2$ profiles are shown in Figure A1. Each galaxy actually has two components with differing ϵ_2: the (dominant) stellar component which reaches its maximum softening length of 0.7 kpc at $z = 1$, and the dark matter component which continues to soften to 1.4 kpc at $z = 0$. Here we show the combined effect of both softenings on the stellar distribution, with the original $z = 2$ profiles in dashed red lines and the softened profiles in dashed green lines. On average, the changing softening length alone results in a change in half-mass radius of about 15% for these galaxies.

REFERENCES

Barnes J. E., 1988, The Astrophysical Journal, 331, 699
Barro G. et al., 2013, The Astrophysical Journal, 765, 104
Barro G. et al., 2014a, The Astrophysical Journal, 791, 52
Barro G. et al., 2014b, The Astrophysical Journal, 795, 145
Belli S., Newman A. B., Ellis R. S., 2014, The Astrophysical Journal, 783, 117
Belli S., Newman A. B., Ellis R. S., Belli ., Newman ., Ellis ., 2014, eprint arXiv:1409.7088, 14
Bezanson R., van Dokkum P. G., Tal T., Marchesini D., Kriek M., Franx M., Coppi P., 2009, The Astrophysical Journal, 697, 1290
Boylan-Kolchin M., Ma C.-P., Quataert E., 2006, Monthly Notices of the Royal Astronomical Society, 369, 1081
Cappellari M. et al., 2009, The Astrophysical Journal, 704, L34
Carollo C. M. et al., 2013, The Astrophysical Journal, 773, 112
Ceverino D., Dekel A., Tweed D., Primack J., 2015, Monthly Notices of the Royal Astronomical Society, 447, 3291
Crain R. A. et al., 2015, eprint arXiv:1501.01311
Daddi E. et al., 2005, The Astrophysical Journal, 626, 680
Damjanov I., Geller M. J., Zahid H. J., Hwang H. S., 2015, eprint arXiv:1501.04976
Damjanov I., Hwang H. S., Geller M. J., Chilingarian I., 2014, The Astrophysical Journal, 793, 39
De Lucia G., Blaizot J., 2007, Monthly Notices of the Royal Astronomical Society, 375, 2
Di Matteo T., Springel V., Hernquist L., 2005, Nature, 433, 604
Dolag K., Borgani S., Murante G., Springel V., 2009, Monthly Notices of the Royal Astronomical Society, 399, 497
Fan L., Lapi A., Bressan A., Bernardi M., De Zotti G., Danese L., 2010, The Astrophysical Journal, 718, 1460
Fan L., Lapi A., De Zotti G., Danese L., 2008, The Astrophysical Journal, 689, L101
Ferré-Mateu A., Mezcua M., Trujillo I., Balcells M., van den Bosch R. C. E., 2015, eprint arXiv:1506.02663
Franx M., van Dokkum P. G., Schreiber N. M. F., Wuyts S., Labbé I., Toft S., 2008, The Astrophysical Journal, 688, 770
Genel S. et al., 2014, Monthly Notices of the Royal Astronomical Society, 445, 175
Graham A. W., Dullo B. T., Savorgnan G. A. D., 2015, The Astrophysical Journal, 804, 32
Hernquist L., 1990, The Astrophysical Journal, 356, 359
Hernquist L., Katz N., 1989, The Astrophysical Journal Supplement Series, 70, 419
Hernquist L., Spergel D. N., Heyl J. S., 1993, The Astrophysical Journal, 416, 415
Hopkins P. F., Bundy K., Hernquist L., Wuyts S., Cox T. J., 2010, Monthly Notices of the Royal Astronomical Society, 401, 1099
Hopkins P. F., Bundy K., Murray N., Quataert E., Lauer T. R., Ma C.-P., 2009a, Monthly Notices of the Royal Astronomical Society, 398, 898
Hopkins P. F., Lauer T. R., Cox T. J., Hernquist L., Kormendy J., 2009b, The Astrophysical Journal Supplement Series, 181, 486
Katz N., Weinberg D. H., Hernquist L., 1996, The Astrophysical Journal Supplement Series, 105, 19
Keating S. K., Abraham R. G., Schiavon R., Graves G., Damjanov I., Yan R., Newman J., Simard L., 2015, The Astrophysical Journal, 798, 26
Mo H. J., Mao S., White S. D. M., 1998, Monthly Notices of the Royal Astronomical Society, 295, 319
Naab T., Johansson P. H., Ostriker J. P., 2009, The Astrophysical Journal, 699, L178
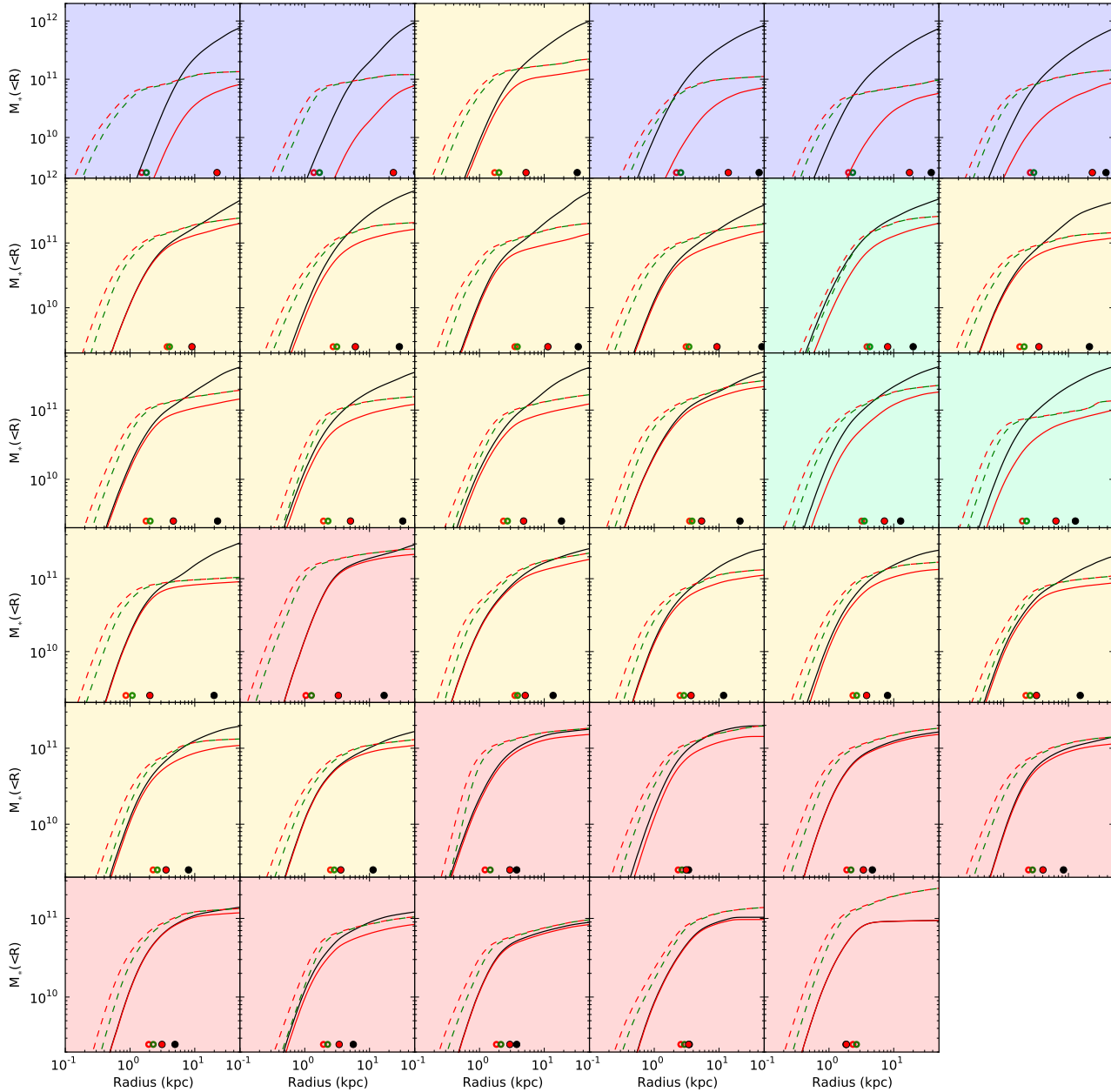
Figure A1. Cumulative stellar mass profiles of compact galaxies, arranged in the same manner as in Fig. 2. *Black solid lines:* Profile of $z = 0$ descendant, including all stars. *Red solid lines:* Profile of $z = 0$ descendant, including only those stars which were a part of the $z = 2$ compact progenitor. The ratio between the red and black solid lines is the quantity f_r discussed in Section 4.1. The background color in each panel indicates the descendant type as in Fig. 3. *Red dashed lines:* Profile of $z = 2$ compact progenitor. *Green dashed lines:* Profile of $z = 2$ compact progenitor when relaxed to $z = 0$ softening lengths. Colored circles at the bottom of each panel mark the half-mass radii of the profiles.

Nelson D. et al., 2015, eprint arXiv:1504.00362

Nelson E. et al., 2014, Nature, 513, 394

Newman A. B., Ellis R. S., Bundy K., Treu T., 2012, The Astrophysical Journal, 746, 162

Newman A. B., Ellis R. S., Treu T., Bundy K., 2010, The Astrophysical Journal, 717, L103

Rahmati A., Pawlik A. H., Raicevic M., Schaye J., 2013, Monthly Notices of the Royal Astronomical Society, 430, 2427

Rodriguez-Gomez V. et al., 2015, Monthly Notices of the Royal Astronomical Society, 449, 49

Saulder C., van den Bosch R. C. E., Mieske S., 2015, eprint arXiv:1503.05117, 37

Schaye J. et al., 2015, Monthly Notices of the Royal Astronomical Society, 446, 521

Sijacki D., Springel V., Di Matteo T., Hernquist L., 2007, Monthly Notices of the Royal Astronomical Society, 380, 877

Sijacki D. et al., 2014, eprint arXiv:1408.6842, 22

Springel V., 2010, Monthly Notices of the Royal Astronomical

Society, 401, 791

Springel V., Di Matteo T., Hernquist L., 2005, Monthly Notices of the Royal Astronomical Society, 361, 776

Springel V., Hernquist L., 2003, Monthly Notices of the Royal Astronomical Society, 339, 289

Springel V., White S. D. M., Tormen G., Kauffmann G., 2001, Monthly Notices of the Royal Astronomical Society, 328, 726

Stringer M., Trujillo I., Vecchia C. D., Martinez-Valpuesta I., 2015, eprint arXiv:1503.03078

Szomoru D., Franx M., van Dokkum P. G., 2012, The Astrophysical Journal, 749, 121

Taylor E. N., Franx M., Glazebrook K., Brinchmann J., van der Wel A., van Dokkum P. G., 2010, The Astrophysical Journal, 720, 723

Torrey P., Vogelsberger M., Genel S., Sijacki D., Springel V., Hernquist L., 2014, Monthly Notices of the Royal Astronomical Society, 438, 1985

Torrey P. et al., 2015, arXiv

Trujillo I., Conselice C. J., Bundy K., Cooper M. C., Eisenhardt P., Ellis R. S., 2007, Monthly Notices of the Royal Astronomical Society, 382, 109

Trujillo I. et al., 2006, Monthly Notices of the Royal Astronomical Society: Letters, 373, L36

Valentinuzzi T. et al., 2010, The Astrophysical Journal, 712, 226

van der Wel A. et al., 2014, The Astrophysical Journal, 788, 28

van Dokkum P. G. et al., 2014, The Astrophysical Journal, 791, 45

van Dokkum P. G., Franx M., 2001, The Astrophysical Journal, 553, 90

van Dokkum P. G. et al., 2008, The Astrophysical Journal, 677, L5

van Dokkum P. G., Kriek M., Franx M., 2009, Nature, 460, 717

van Dokkum P. G. et al., 2006, The Astrophysical Journal, 638, L59

van Dokkum P. G. et al., 2015, eprint arXiv:1506.03085

Vogelsberger M., Genel S., Sijacki D., Torrey P., Springel V., Hernquist L., 2013, Monthly Notices of the Royal Astronomical Society, 436, 3031

Vogelsberger M. et al., 2014a, Monthly Notices of the Royal Astronomical Society, 444, 1518

Vogelsberger M. et al., 2014b, Nature, 509, 177

Wellons S. et al., 2015, Monthly Notices of the Royal Astronomical Society, 449, 361

Wiersma R. P. C., Schaye J., Smith B. D., 2009, Monthly Notices of the Royal Astronomical Society, 393, 99

Wiersma R. P. C., Schaye J., Theuns T., Dalla Vecchia C., Tornatore L., 2009, Monthly Notices of the Royal Astronomical Society, 399, 574

Williams C. C. et al., 2014, The Astrophysical Journal, 780, 1

Zolotov A. et al., 2015, Monthly Notices of the Royal Astronomical Society, 450, 2327